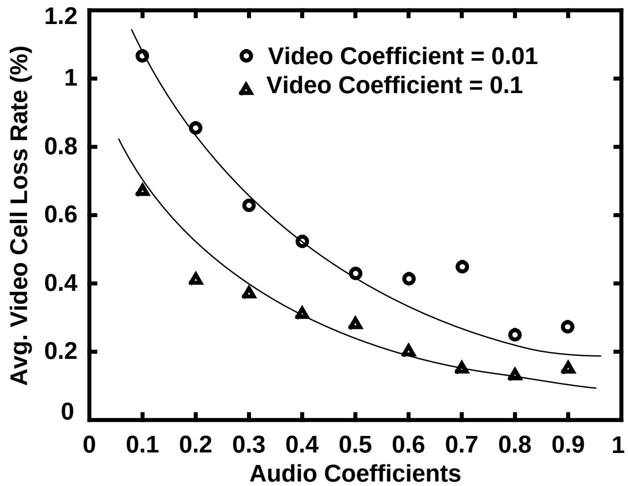

Fig. 6. The average video cell loss rate as a function of audio coefficients

and an increase in maximum data queue length for the lowest delay priority data traffic cells.

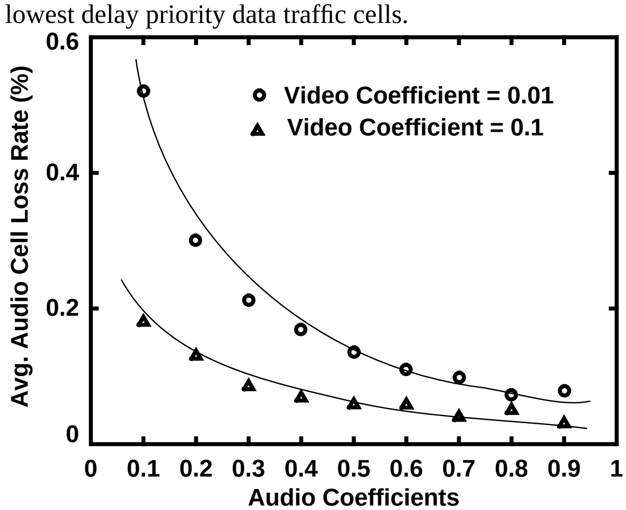

Fig. 7. The average audio cell loss rate as a function of video buffer sizes for an ATM network with output.

5 Conclusion

In order to test various admission control and routing algorithms proposed for ATM networks using different traffic models and topologies, we have developed a modular ATM network simulator that allows us to "plug and play" with various components and parameters of the system. We have implemented an admission control algorithm based on the effective bandwidth concept, and evaluated the network performance using a wide variety of parameter settings. Using simulation methods we studied the relationships between switch buffer size, admission control schemes and the maximum queue length. Our results demonstrated that the simple admission scheme we implemented is effective.

Acknowledgments

We would like to thank Prof. Domenico Ferrari, University of California at Berkeley for his valuable suggestions. We also would like to thank Matthew Brundjar who assisted in building the ATM network simulator, and Ning Xiao who helped to design the general architecture of the simulator. We wish to acknowledge the support of Pacific Gas & Electric Company, which funded our NetPlan research project, the basic environment for the current ATM network simulation platform.

References

[1] H. Ahmadi and W. Denzel, "A Survey of Modern High-Performance Switching Techniques", *IEEE J. Selected Areas in Communication,* vol. SAC-7, 1989, pp. 1091-1103.

[2] G. R. Ash, J. Chen, A. E. Frey, B. D. Huang, C. Lee and G. L. McDonald, "Real-Time Network Routing in the AT&T Network - Improved Service Quality at Lower Cost", *Proc. IEEE GLOBECOM '92*, Orlando, FL, Dec. 1992, pp. 802-809.

[3] J. Buck, E. E. Goei, S. Ha, I. Kuroda, P. Lapsley, E. A. Lee and D. G. Messerschmitt, *ALMAGEST: The Ptolemy User's Manual*, University of California, Berkeley, CA, 1991.

[4] H. J. Chao and N. Uzun, "An ATM Queue Manager with Multiple Delay and Loss Priorities", *Proc. IEEE GLOBECOM '92*, Orlando, FL, Dec. 1992, 308-313.

[5] Z. Dziong, J. Choquette, K. Liao and L. Mason, "Admission Control and Routing in ATM Networks", *Computer Networks and ISDN Systems 20*, 1-5 (Dec. 1990), 189-196.

[6] Shau-Ming Lun, Felix Wu, Ning Xiao, Pravin Varaiya, "NetPlan: An Integrated Network Planning Environment", *State of the Art in Performance Modeling and Simulation: Computer and Communication Networks,* Vol.1, Kluwer Academic Publisher, 1993.

[7] G. Kesidis and J. Walrand, "Effective Bandwidths for Multiclass Markov Fluids and Other ATM Sources", UCB/ERL Tech. Rep. M92/40, Univ. of California, Berkeley, CA, Apr. 1992.

[8] J. Turner, "Managing Bandwidth in ATM Networks with Bursty Traffic", *IEEE Network 6*, 5 (Sep. 1992), 50-58.

[9] Y. S. Yeh, M. G. Hluchyi and A. S. Acampora, "The Knockout Switch: A Simple, Modular Architecture for High-Performance Packet Switching", *IEEE J. Selected Areas in Communications SAC-5*, 7 (Oct. 1987), 1274-1283.

[10] B. Maglaris, D. Anastassiou, P. Sen, G. Karlsson, and J. Robbins, "Performance Models of Statistical Multiplexing in Packet Video Communications," *IEEE Transactions on Communications*, vol. 36, pp. 834-844, 1988.

[11] L. Kleinrock, *Queuing Systems*, vol. 1, New York: Willey, 1975.

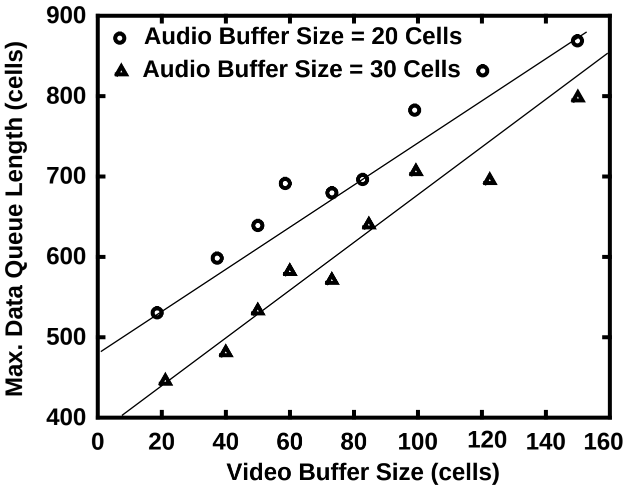

Fig. 2. The maximum data queue length as a function of video buffer size

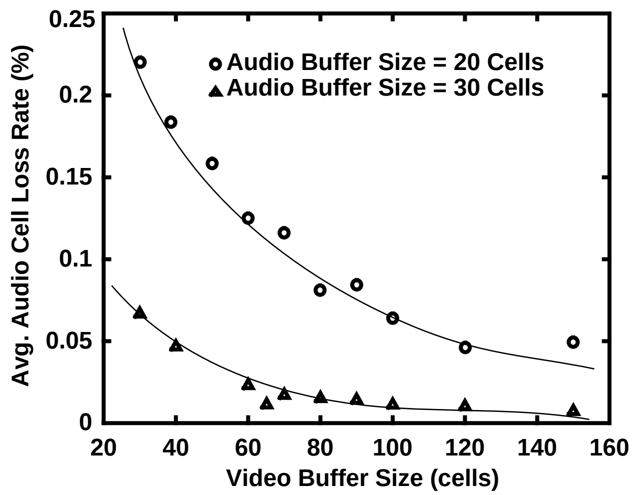

Fig. 4. The average audio cell loss rate as a function of video buffer sizes

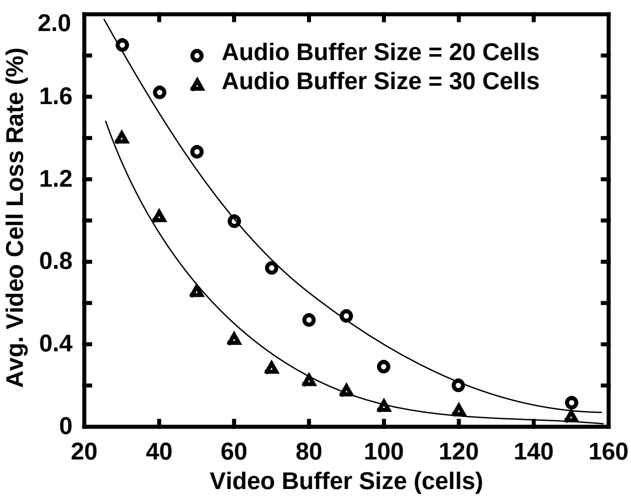

Fig. 3. The average video cell loss rate as a function of video buffer size.

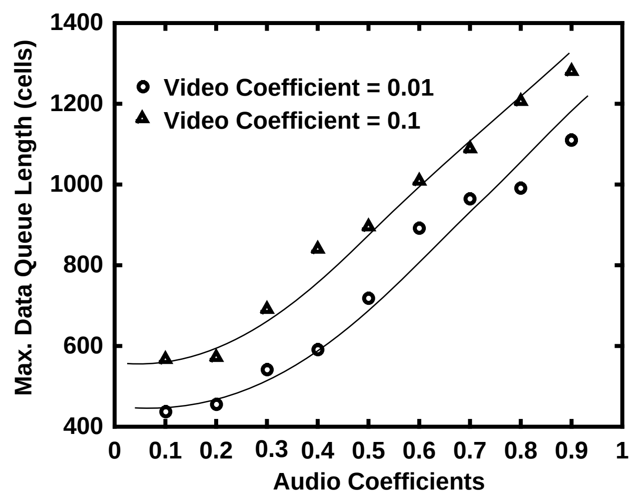

Fig. 5. The maximum data queue length as a function of audio coefficients

observed to decrease as the buffer size increases. Furthermore, the cell loss rate is lower for larger audio buffers since more audio/video traffic can be served.

A number of simulations were performed using various combinations of admission control coefficients for calculating the effective bandwidth of the traffic. The maximum queue length for the data cells and the average cell loss rate for the video and audio cells were calculated from the simulation results. In the simulations, each of the three types of traffic has an average bandwidth of 16 Mbits/sec. The buffer sizes for the audio and video traffic are 20 cells and 60 cells, respectively.

Fig. 5 shows the maximum data queue length as a function of the audio coefficient. As the value of the audio coefficient increases, the maximum data queue length increases. Fig. 6 and Fig. 7 illustrates the average cell loss rate as a function of audio coefficient for video traffic and audio traffic, respectively. The average cell loss rates for video and audio traffic decrease as the corresponding coefficients increase.

These phenomena are attributed to the manner in which admission control coefficients were assigned to the three types of traffic. To guarantee the QOS for realtime traffic, higher admission coefficients were assigned to the audio cells. As the admission control coefficient is increased, the cell drop rate for the realtime traffic decreases, while the maximum queue length for the non-realtime traffic increases. This is due to the fact that increasing *Coeff* results in a larger amount of bandwidth allocated to realtime traffic; hence, a lower cell drop rate drop), buffer sizes and a control variable for some well-known traffic sources (e.g., Poisson, Gaussian, renewal, Markov fluids). We introduce the concept of effective bandwidths below.

Let α_j be the effective bandwidth of a type *j* source. According to [7], under suitable mixing conditions, the effective bandwidth α_j of a type *j* source can be expressed as

$$\alpha_j(\delta) = \frac{\Lambda_j(\delta)}{\delta}. \tag{5}$$

where

$$\Lambda_j(\delta) = \lim_{t \to \infty} \frac{1}{t} \log E\{\exp[\delta \Lambda_j(t)]\} \tag{6}$$

and δ is a small number related to the cell drop rate.

For an identical independent (i.i.d.) Poisson process with

$$A(t) = X_1 + X_2 + \ldots + X_t, \tag{7}$$

where X_j is a i.i.d. Poisson random variable,

$$\Lambda_j(\delta) = \log E\{\exp[\delta X_j]\} = \lambda_j[\exp(\delta) - 1], \tag{8}$$

where λ is the average traffic bandwidth. δ is defined as the *admission control coefficient (Coeff)* which is determined by the user. Thus, the effective bandwidth of a type *j* source can be expressed as

$$\alpha_j(\delta) = \frac{\lambda_j[\exp(\delta) - 1]}{\delta}. \tag{9}$$

The switch refuses a connection request if the calculated effective bandwidth exceeds the remaining bandwidth on the selected output link, or the estimated delay recorded in the setup cell plus the expected delay at this switch exceeds the maximum delay. Each switch estimates its delay as the mean switch fabric processing time plus a delay based on the time-averaged output queue length.

4 Experimental Results

4.1 The Experimental ATM Network

The experimental ATM network topology is shown in Fig. 1. Each arrow represents a transmission line with a full-duplex bandwidth of 155Mbits/sec and one of a variety of propagation delays. Switch-switch propagation delays are on the order of 10 μs, while host-switch line delays are on the order of 1 μs.

4.2 Issues for Experimentation

For realtime services, delay is the primary performance requirement, while for non-realtime services, reliability is the foremost concern. To satisfy these two

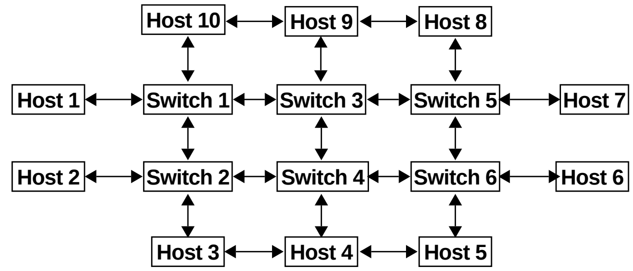

Fig. 1. The experimental ATM network topology.

different requirements, the control scheme used in the simulations gives higher scheduling priority to realtime traffic, and low priority to non-realtime traffic. However, there is no preemptive function, due to the very small ATM cell size. To increase the reliability of the data transfer services, large buffer sizes are used. The issues we investigated are listed below:

- The relationship between buffer size and cell loss rate.
- The maximum buffer size needed to guarantee a low cell loss rate for data transfer.
- The effect of different coefficients for effective bandwidth calculations on overall network performance (e.g., cell loss).

Because limiting the realtime buffer size places hard bounds on the maximum delay, and transmission and propagation delay are very small in high-speed networks, the end-to-end delay is relatively insignificant in our network, and its effects were not examined in this paper.

4.3 Results and Analysis

A number of simulations using various combinations of audio and video buffer sizes were performed. Each of the three types of traffic had an average bandwidth of 16 Mbits/sec, and the admission control coefficients for audio, video and data were set at 0.5, 0.1 and 0.01, respectively. The network performance was evaluated in terms of audio/video cell loss rate and maximum data queue length.

Fig. 2 illustrates the maximum data queue length as a function of video buffer size. As the video buffer size increases, the maximum data queue length increases. The reason for this phenomenon is due to our scheduling scheme: when more realtime traffic is present in the network, data cells must wait in the buffer for a longer period of time before being served. Note that the maximum data queue length is larger for smaller audio buffer size values which correspond to smaller end-to-end delays for the realtime traffic and thus, higher throughput (the number of cells per second).

Fig. 3 and Fig. 4 show the cell loss rate as a function of video buffer size for video traffic and audio traffic, respectively. From these two figures, the cell loss rate is video traffic is modeled as a first-order autoregressive Markov process, as described below [10].

Let $\lambda(n)$ represent the bit rate of a single video source during the *n*th frame. A first-order autoregressive Markov process $\lambda(n)$ is generated by the recursive relation:

$$\lambda(n) = a\lambda(n-1) + b\omega(n), \tag{1}$$

where $\omega(n)$ is a sequence of independent Gaussian random variables, and *a* and *b* are constants. Assume that $\omega(n)$ has mean η and variance 1. Further assume that $|a| < 1$; thus, the process achieves steady state with large *n*. The steady-state average $E(\lambda)$ and discrete autocovariance $C(n)$ are given by [11]

$$E(\lambda) = \frac{b}{1-a}\eta. \tag{2}$$

$$C(n) = \frac{b^2}{1-a^2}a^n. \tag{3}$$

Based on the experimental data from [10], $E(\lambda) = 0.52$ bits/pixel and $C(n) \approx 0.0536 \times (e^{-0.13n})$ $(\text{bits/pixel})^2$. Comparing the coefficients in (2) and (3), we obtain

$$a \approx 0.8781 \qquad b \approx 0.1108 \qquad n \approx 0.572. \tag{4}$$

In our simulations, we assumed that the transmitted video packets are signals from video conferences; the video source generates 30 frames/sec, and there are 352×288 pixels/frame. If the mean number of bits/pixel $E(\lambda)$ is 0.52, then the average bit rate of the video traffic is equal to 1.5 Mbits/sec. Video packet and frame lengths are assumed equal, each with an average length of 6.8 kbytes. The service time for each video packet is a deterministic value equal to 33.33 msec.

3 Routing and Admission Control

3.1 Routing Algorithm

Routing is a central issue in ATM networks. Many routing algorithms which have been developed for circuit-switched networks can be applied to ATM networks. In many cases it is desirable for the routing algorithm to consider the current link utilization before a decision is made. Some systems use a *least-loaded path* approach in which calls are routed onto the path with the maximum residual capacity [2]. Other methods include a state-dependent algorithm which uses a *reward maximization* scheme [5]. In our design, we used a least-hop-count depth-first search method, because of its simplicity and its adaptability to congestion conditions.

The routing algorithm adopted in this study consists of a depth-first search of the network, rooted at the switch directly connected to the source host. The algorithm successively attempts to reach the destination through each link by trying the one with the smallest hop count first. Our rationale for not using something more complex is that (1) most propagation delays along a given host's links are likely to be of the same order of magnitude, and (2) any gateway links (long-haul connections) are unlikely to lead back to the local network because we limit the total path length.

In order to limit the total path length while still allow the use of suboptimal paths, we restrict the depth of the search to no more than k times the hop count known to the root switch. In our simulations, k=2 was chosen as the default value, because a path that utilizes anything worse than the second-best path is likely to be a poor choice. This default value (1) limits the amount of time the network spends searching for virtual paths and (2) improves resource utilization by reducing the number of “bad” paths found, at the expense of not considering usable paths.

3.2 Admission Control Algorithm

An open and challenging problem for high speed networks is the allocation of bandwidth to various services, such that certain grades of service, e.g., delay constraints and loss probabilities, are satisfied, and reasonable network utilization is achieved. A brief survey of several popular bandwidth allocation schemes is given below [8].

In *peak rate allocation*, incoming calls specify the maximum rate at which they will enter the network. The major disadvantage is the wasted bandwidth due to the bursty nature of the traffic. In *minimum throughput allocation*, calls are guaranteed a percentage of the link bandwidth when the switch is congested, and may exceed this amount when the link is not as busy. The sum of the allocated throughputs is limited to the link bandwidth, and cells will be discarded if the switch is congested. A limitation of this approach is that it relies on *a priori* knowledge of the bandwidth requirement of each incoming call, which may be unavailable. Another alternative, a variant of the leaky bucket method, uses the specified values of peak and average cell rates, along with maximum burst size. Although its implementation is somewhat complex, this method attempts to balance performance guarantees and link utilization [8].

One drawback of using the methods above is that the relationship between the quality of service and admission control scheme is not explicitly given. To deal with this problem, the concept of effective bandwidth may be applied to the admission control algorithm [7]. The effective bandwidth of a traffic source is dependent only on the traffic and the acceptable loss probability. Based on the effective bandwidth, one can calculate the (minimum) channel capacity needed to maintain a certain grade of service for a single switch. Kesidis, *et al.* [7] derived the relationships between the probability of buffer overflow (cell

An ATM Network Simulator to Study Admission Control and Routing Algorithms

Zhigang Qin, Wendy Wang*, Felix Wu, Paul Aoki, Tetiana Lo

Department of Electrical Engineering and Computer Sciences
University of California, Berkeley, CA 94720

Abstract

We have developed an Asynchronous Transfer Mode (ATM) network simulator to study the relationships between switch buffer sizes, admission control schemes and maximum queue length of an experimental network. The simulations are performed at the ATM cell level. Traffic generators, network interfaces, and switching elements are coded as modular building blocks which allow us to evaluate network performance using different traffic models, switch configurations and network topologies. Our results demonstrate the effectiveness of our proposed admission control scheme based on the concept of effective bandwidth.

Keywords: ATM, admission control, routing algorithms, network simulation.

1 Introduction

After years of extensive research, many important aspects of Asynchronous Transfer Mode (ATM) networks (such as admission control and routing algorithms) remain largely undecided. Because of the complexity of ATM networks, the "best" choice is not always obvious, and many proposed admission control algorithms based on analytical methods rely on unrealistic assumptions, such as a network with exactly one switch or a single traffic source.

We believe that simulation provides the only viable tool to understand and compare the performance of the proposed protocols and algorithms used in ATM networks. Therefore, we have constructed an ATM network simulator, one that is flexible and modular, to allow experimentation with different algorithms and parameters, and to address relevant ATM network issues such as call admission control policies and virtual circuit routing. This simulator has been used to generate experimental results which correspond to the expected behavior of an ATM network using an admission control algorithm with various parameter settings.

2 Implementation of the ATM Simulator

The ATM network simulator was implemented using the Ptolemy simulation environment [3], as an extension of our work on NetPlan[6]. Ptolemy provides many advantages for rapid simulator development: (1) a framework for writing and coordinating independently-scheduled basic blocks called *star*s, (2) message-based communications primitives and (3) flexible mechanisms for event scheduling. These features make Ptolemy well-suited for network simulation. Because the subjects of our study, the routing and control algorithms, operate at the cell level, the simulator is implemented at the cell level, and each layer in the ATM model is implemented as a separate star to make the simulator flexible.

2.1 The Switch Model

The current implementation of our ATMSwitch star models a switch fabric with *disjoint-path topology and output queueing*, an example of which is Knockout [9]. This type of switch is designed to handle the maximum aggregate input traffic rate, so that no input queuing (and consequently, head-of-the-line blocking) occurs. For this reason, such non-blocking space-division fabrics provide the best delay/throughput performance, given sufficient space in the output queue [1].

Our switch star assumes one additional facility: prioritization of realtime and non-realtime traffic ([4] describes a switch based on similar ideas). Realtime traffic is always transmitted before non-realtime traffic. The non-realtime output queue is set to infinite length, assuming that (in practice) the switch buffering memory will be adjusted to produce the maximum tolerable data cell loss rate. The realtime output queue has a fixed buffer size to place a hard limit on the maximum queuing delay imposed by the ATM switch on realtime traffic.

2.2 Traffic Source Model

Three types (audio, video, and data) of traffic sources have been implemented. The audio traffic is modelled as a Poisson process; the lengths and interarrival times of each audio packet are exponentially distributed. The number of audio packets transmitted during a connection is a random variable. After a talk session, the system waits a random time and then begins a new audio transfer. The data source is modelled similarly as the audio traffic, aside from the parameter values.

Because variable bit rate video coders exhibit continuous variations in the output, modeling the video source as a Poisson process would have been inappropriate. Instead,

* currently at Rockwell International Co., 4311 Jamboree Rd., Newport Beach, CA 92658.